Airway-Tree Segmentation in Subjects with Acute Respiratory Distress Syndrome

Kristína Lidayová[1(✉)], Duván Alberto Gómez Betancur[4], Hans Frimmel[2], Marcela Hernández Hoyos[4], Maciej Orkisz[5], and Örjan Smedby[3]

[1] Division of Visual Information and Interaction, Centre for Image Analysis, Uppsala University, Uppsala, Sweden
kristina.lidayova@it.uu.se
[2] Division of Scientific Computing, Department of Information Technology, Uppsala University, Uppsala, Sweden
[3] School of Technology and Health, KTH Royal Institute of Technology, Stockholm, Sweden
[4] Systems and Computing Engineering Department, School of Engineering, Universidad de Los Andes, Bogotá, Colombia
[5] CREATIS UMR 5220, U1206, CNRS, Inserm, INSA-Lyon, Université Claude Bernard Lyon 1, UJM-Saint Etienne, Univ. Lyon, 69621, Lyon, France

Abstract. Acute respiratory distress syndrome (ARDS) is associated with a high mortality rate in intensive care units. To lower the number of fatal cases, it is necessary to customize the mechanical ventilator parameters according to the patient's clinical condition. For this, lung segmentation is required to assess aeration and alveolar recruitment. Airway segmentation may be used to reach a more accurate lung segmentation. In this paper, we seek to improve lung segmentation results by proposing a novel automatic airway-tree segmentation that is able to address the heterogeneity of ARDS pathology by handling various lung intensities differently. The method detects a simplified airway skeleton, thereby obtains a set of seed points together with an approximate radius and intensity range related to each of the points. These seeds are the input for an onion-kernel region-growing segmentation algorithm where knowledge about radius and intensity range restricts the possible leakage in the parenchyma. The method was evaluated qualitatively on 70 thoracic Computed Tomography volumes of subjects with ARDS, acquired at significantly different mechanical ventilation conditions. It found a large proportion of airway branches including tiny poorly-aerated bronchi. Quantitative evaluation was performed indirectly and showed that the resulting airway segmentation provides important anatomic landmarks. Their correspondences are needed to help a registration-based segmentation of the lungs in difficult ARDS cases where the lung boundary contrast is completely missing. The proposed method takes an average time of 43 s to process a thoracic volume which is valuable for the clinical use.

Keywords: Airway segmentation · Airway-tree centerline detection · Thoracic CT · ARDS

P. Sharma and F.M. Bianchi (Eds.): SCIA 2017, Part II, LNCS 10270, pp. 76–87, 2017.
DOI: 10.1007/978-3-319-59129-2_7

1 Introduction

Acute Respiratory Distress Syndrome (ARDS) is a life-threatening respiratory condition. This syndrome may occur as a consequence of a major injury or different pulmonary aggressions (bacteriological or chemical). As a result, the lungs are unable to fill with air and cannot provide enough oxygen into the bloodstream. The treatment requires the use of mechanical ventilation to pump air into the patient's lungs until the cause of the disease is detected and treated. Mechanical ventilator parameters (tidal volume and positive end-expiratory pressure - PEEP) need to be set carefully, taking into account the patient's clinical condition. Too large air volumes or too high PEEP may injure the lungs. On the other hand, lack of oxygen in the blood may lead to a multiple organ dysfunction syndrome. Both cases are with fatal consequences. Knowledge about the lung aeration is the key to helping prevent the injury. Since gray levels in Computed Tomography (CT) images are associated with the tissue density, thoracic CT scans are well suited to obtain this knowledge. Nevertheless, the accuracy of lung aeration quantification is hampered by two factors: the difficulty in delineating the outer boundary of the lungs (due to local lack of contrast), and the inclusion of internal structures not belonging to the parenchyma, such as the airway tree. To cope with both problems, airway segmentation can be useful. It can provide anatomic landmarks useful in lung delineation, and it can also serve for airway removal.

Airway segmentation is confronted with specific difficulties related to variable contrast in CT images from subjects with ARDS. In deflated lungs with low PEEP condition, the large opacities of non-aerated parenchyma make it very difficult, if at all possible, to see the lung boundary. Also, small bronchi are thinner in this condition. At the other extreme, when lungs are strongly inflated, the problem is mainly caused by a low contrast between the parenchyma and bronchi lumen. For smaller bronchi, the thickness of the wall may be below the scan resolution and can cause the segmentation algorithms to leak into the parenchyma. Bronchi filled with liquid or mucus seem to be disconnected on the CT scan, which presents another complication, mainly for segmentation algorithms based on a region-growing or wave propagation.

In this paper, we propose a novel airway-tree segmentation method that successfully deals with the challenges brought by ARDS. The method detects an approximate airway centerline tree and then applies the obtained intensity and distance information to restrict the onion-kernel region-growing segmentation and prevent it from leaking into the parenchyma. The method was evaluated on a series of thoracic CT images of subjects with ARDS, acquired at significantly different mechanical-ventilation conditions. The results show that the proposed method is able to find a large number of branches including tiny bronchi. This is important for achieving our overall goal - the improvement of the lung segmentation - especially in low PEEP conditions where the lung boundary contrast is missing. A possible approach is to use a self-atlas segmentation. It consists in segmenting the lungs in the most-contrasted volume and warping them towards the least-contrasted one by means of registration. In this work, we confirmed that

using a hybrid registration that combines airway-tree landmark correspondences obtained from the segmented airway tree with gray-level information leads to an improvement in the lung segmentation. In addition, the proposed method is fast, which is valuable for clinical use.

2 Related Work

The segmentation of airway trees plays an important role in the analysis of various lung diseases. Since each disease brings its own challenges, specifications, and restrictions, there exist many different methods for airway-tree segmentation. An intuitive approach is based on a 3D region-growing [1–3] and relies on the contrast between the airway lumen and the airway wall that is usually relatively high. However, due to noise or partial volume effect, the contrast may be missing and the region-growing segmentation may leak into the parenchyma. Algorithms applying region-growing differ in the way they prevent the leakages. Many algorithms use region-growing only for large airways and implement additional procedures to identify smaller airways. A review work of Pu et al. [4] provides a division of other methods for airway segmentation into five categories based on their methodology as follows:

Morphological methods [5] use morphological reconstruction techniques to identify airways on CT slices and then reconstruct them as a connected 3D airway tree. Nevertheless, the reconstruction largely depends on how continuous the detected airway candidates are in space.

Knowledge-based methods [6] identify the airways by using various anatomical knowledge and rules. Since it is hard to list all the rules that characterize the airways, these methods are often used in combination with other approaches and remove false positives rather than detect the true positives.

Template matching methods [7] search for airway regions that match a set of predefined elliptical (2D) or tubular (3D) templates. Just like with the previous category, the main problem is to list all the templates that would fully describe the airways together with their size variability.

Machine learning methods [8] automatically learn specific airway characteristics during the training process. However, the diversity of the pre-labelled training data and the feature selection are critical for the final performance.

Geometric shape analysis methods [9] make use of Hessian-matrix based filters for tubular shape detection. However, these filters are sensitive to noise and irregularities caused by diseases. In addition, Gaussian convolution filter may blur small airways.

A summary and comparison of 15 different airway-tree segmentation methods can be found in the EXACT'09 challenge [10]. Each of the algorithms has its advantages and disadvantages. From the published results, it is evident that there is no one algorithm solving all application challenges. Therefore, we propose a method focused on subjects with ARDS. The method can be categorized as a knowledge-based method combined with 3D region-growing. A detailed description of the proposed method follows in the next section.

3 The Proposed Method

The proposed method takes a thoracic CT volume as an input. Since airways appear as elliptical regions on orthogonal CT image slices, our method uses knowledge-based filters to identify central voxels of these regions - the graph nodes. These nodes can represent bifurcating airways, as well as end or line points of the airway. There is no need to detect every single airway central voxel – a sparse detection is satisfactory. The distance between the central voxels (detected nodes) is, in general, longer for thicker airways and much shorter (only 1–2 voxels) for thinner ones which safely detects also curved branches. The nodes are then connected with straight edges into a tree graph structure representing the approximate centerline tree of the airway. The connection process is controlled by a set of criteria to ensure that the edges lie inside the airway tree and loops are avoided. The approximate centerline tree serves as a sufficient input for the subsequent segmentation algorithm. The complete centerline tree is voxelised, and for each voxel, information about its position, expected radius and an intensity range related to the position is stored. This information is important to prevent leakage into the parenchyma. Each voxel is then used as a seed point in a modified region-growing algorithm, which generates as output a binary segmentation of the airway tree. The pipeline of the whole algorithm is visualised in Fig. 1. In the following subsections, we describe the centerline tree extraction and segmentation algorithms more in detail.

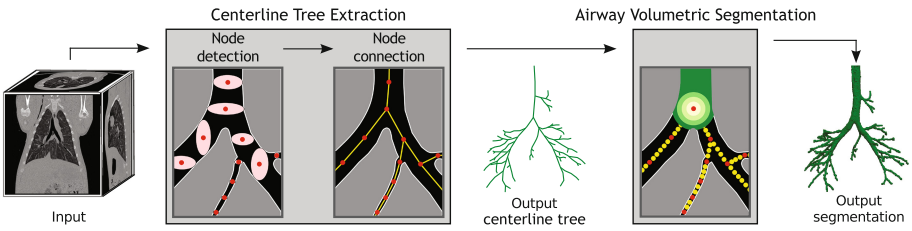

Fig. 1. Algorithmic overview. From input CT volume, a centerline tree is extracted in two steps, followed by airway segmentation based on region growing.

3.1 Centerline Tree Extraction Algorithm

The basic centerline tree extraction algorithm is based on an idea presented in [11]. However, it has been modified and extended for the needs of airway-tree centerline detection. Since airways are filled with air, potential graph nodes - voxels of interest - are expected to be aerated. Furthermore, the morphology of a lung suffering from the ARDS is very heterogeneous, it is meaningful to divide these potential voxels of interest into classes based on their physical density and to treat each of the classes differently. In literature, voxels in the parenchyma are divided based on their physical density into four aeration classes [12].

The denser the tissue inside the voxel, the higher the X-ray attenuation, which results in a higher gray level value (CT number). The gray level values are expressed in Hounsfield units (HU). Pure air voxels are assigned values of –1000 HU (no attenuation), whereas pure water voxels have values of 0 HU. Since tissues are mainly composed of water, their typical density is close to that of water. The four aeration classes then are:

- **Over-aerated voxels** [–1024, –900) HU may be found in over-distended parenchymal regions of mechanically ventilated lungs; in normal lungs, voxels with densities from this range are located mainly inside the largest airways.
- **Normally aerated voxels** [–900, –500) HU, in case of healthy subjects, are mostly located in parenchyma or can be located in thin airway bronchi, where the partial volume effect causes the rise in their intensities. In subjects suffering from ARDS, bronchi can be partly filled or completely blocked by mucus or liquid, which may increase the density even in the thick bronchi.
- **Poorly aerated voxels** [–500, –100) HU are usually observed in diseased parenchyma affected by ARDS, but gray levels from this range may also occur in tiny bronchi.
- **Non-aerated voxels** [–100, 100) HU, as the name of the class specifies, correspond to parenchymal regions that do not contain any air. These voxels may also correspond to structures like airway wall or vessels.

The potential graph nodes should be within the range [–1024, –100) HU which corresponds to the intensity ranges of the three aerated classes defined for the parenchyma. The parenchyma of sick subjects is very heterogeneous and can contain voxels of all kind of aeration. As it is possible to see from the class description, the voxels that fit within the intensity range of our interest are potential graph nodes present, either inside the airway tubes or in the parenchyma. Therefore, some filters to distinguish between the true and false airway voxels are needed. The rules are introduced in the following subsections where a further description of the detection and connection steps are provided.

Node Detection. The input volume is analysed through all slices in the three axis-oriented directions (axial, sagittal and coronal). In each slice, if a voxel has the intensity within the range [–1024, –100) HU, it is considered as a potential airway node. Such voxel needs to be examined further by looking into the intensities of surrounding voxels from the same slice. First, the position of the candidate voxel must be confirmed to be central within the lumen. This is done by casting rays in four main directions (up, down, left and right) starting from the candidate voxel position outwards until they reach a lumen border. The lumen border is defined as the first of n consecutive voxels of intensity higher than I, where I is either the upper bound of the aeration class where the candidate voxel belongs or intensity of the candidate voxel increased by 100 HU, whichever of them is higher. This offers an overlap if the candidate voxel intensity is similar to the higher bound intensity. If the two vertical distances and the two horizontal distances to the lumen border are pairwise equal, then these

distances are saved as a major (a) and a minor (b) axis of a bounding ellipse. If the length of these two axes falls outside the specified minimum and maximum allowed radius, then the candidate voxel is discarded. In a subsequent step two auxiliary ellipses - inner and outer - are introduced. Both ellipses share the same center with the bounding ellipse and lie in the same slice, but have different axis lengths. They are shorter by x (inner ellipse) and longer by y (outer ellipse) pixels than the bounding ellipse axes. By subtracting the average intensity of voxels on the inner ellipse from the average intensity of voxels on the outer ellipse, we check if the region supposed to be the lumen is sufficiently darker than its wall. The difference, how much darker the inside should be, compared to the outside, is a function of a radius. The radius, $r = \sqrt{ab}$, is calculated from the major and minor axes as an area-preserving transformation from an ellipse to a circle. For bigger radii, the difference should be larger than for smaller radii since we expect that bigger bronchi are less affected by the partial-volume effect, as well as by physiological-liquid blockages, than smaller bronchi. The nodes that pass the complete set of filters are saved together with information about position, intensity and radius. Table 1 summarises the values for all the parameters.

Table 1. Parameters used in the algorithm listed with their corresponding values

Parameter name	[–1024, –900) HU	[–900, –500) HU	[–500, –100) HU
n number of border voxels	3	2	1
min_radius	1 mm	limited by the voxel size	limited by the voxel size
max_radius	20 mm	5 mm	3 mm
x voxels shorter	1	1	1
y voxels longer	2	1	0
max_edge_length	35 mm	10 mm	5 mm

Node Connection. In this step, the previously detected graph nodes are connected into a graph structure. Starting with each node considered as a separate graph, the graphs are gradually merged by adding links between them. A link between two nodes can be created only if the straight-line connection is shorter than *max_edge_length* (See Table 1), and lies within the airway lumen, *i.e.*, if all voxels intersected by the connection line have intensities within the range [–1024 HU, L), where L is the upper bound of the aeration class corresponding to the brighter of the two connected nodes. If the two nodes are already part of the same graph (connected via other nodes), or if there exists another node at a closer distance that fulfills the conditions, then the connection is not established. After all possible connections have been created, one or more approximate airway centerline trees represent the result. In situations when the bronchi contain mucus, the detected centerline trees are disconnected. The mucus consists mainly of liquid and therefore the corresponding intensity is outside the aerated range. Based only on the distance and the intensity, it is not possible to decide whether

the connection passes through the mucus (and should be part of bronchi) or through the parenchyma (and should not be part of bronchi). Therefore, centerline trees of bronchi filled with liquid or mucus are left disconnected but not removed. If only one resulting tree is desired, all centerline trees not connected to the biggest centerline tree are removed.

3.2 Airway Segmentation

The approximate centerline tree is an important input for the modified onion-kernel region-growing algorithm, originally proposed for use in colon segmentation [13]. The centerline tree consists of nodes that contain information about their position, the airway radius and the intensity range in which the nodes have been detected. Now, the linear edge connections need to be voxelised and the node information interpolated for all the voxels on the line between two nodes. All these voxels become seeds for the region-growing algorithm. Since airway-tree segmentation is challenging mainly because the parenchyma has intensities very similar to those inside the airway, and the airway wall is often disconnected on several places, the region growing algorithm uses the information about the airway radius and intensity to stop the leakage. The region growing can not propagate further than twice the radius at the seed point. Furthermore, only voxels within the intensity range [–1024 HU, L) - where L is again the upper bound of the aeration class corresponding to the brighter of the two connected nodes - should be included in the segmentation.

The onion-kernel region-growing algorithm itself is similar to classical region growing (26 neighbours). However, in the onion kernel case the growing is performed in layers from the seed point outwards (inverse onion peeling). First, the seed voxel is automatically included in the segmentation and is considered to be a zero layer. Then, all voxels from the first layer (1 voxel away from the seed) are processed. One voxel is included in the segmentation if it meets the intensity-based inclusion criterion and is 26-connected with at least one voxel from the previous layer that is already part of the segmentation. Afterward, all voxels which are 1 voxel further from the seed than the voxels considered in the previous step, are processed. This repeats until the distance from the seed point

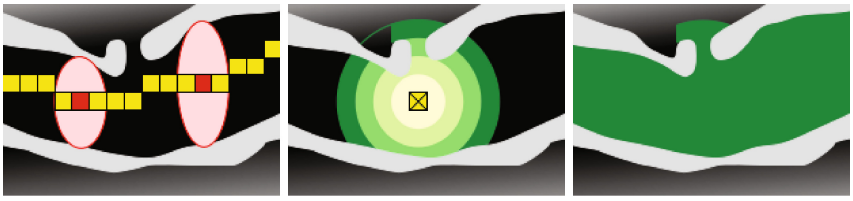

Fig. 2. Onion-kernel region-growing, (a) the input centerline tree is voxelised, (b) each centerline tree voxel becomes a seed; the segmentation is not allowed to grow backwards to fill the cavities (the dark green border delineates the region that would be filled otherwise, (c) the final segmentation. (Color figure online)

reaches twice the radius. The reasoning behind this inverse onion peeling is to achieve locally convex segmentation without segmentation "overhangs". Figure 2 shows the advantage of the inverse onion peeling propagation.

4 Evaluation and Results

We evaluated the proposed method, both qualitatively and quantitatively, using real 3D thoracic CT volumes of piglets with ARDS induced. The qualitative comparison was performed against a reference method based on region-growing and introduced by Mori et al. [1]. The quantitative evaluation tested if the goal of our work - to improve the lung segmentation by use of the airway-tree segmentation - is fulfilled.

4.1 Dataset

For each piglet, several 3D image pairs (end-inspiration/end-expiration) were acquired at various volume and pressure settings. For the qualitative evaluation two piglets were chosen, providing 35 image pairs, resulting in a total of 70 thoracic CT volumes that were processed. For the quantitative evaluation, large displacements and density changes between the analysed volumes are the most challenging and, therefore, three images acquired in end-inspiration at extreme and intermediate PEEP values – 20, 10, and 2 cmH_2O, with a constant tidal volume $V_t = 5$ ml/kg – were chosen.

4.2 Qualitative Evaluation

The reference segmentation method used for a visual comparison of the results is commonly referred to be a benchmark within the airway segmentation methods. It is simple and fast, and it avoids leakages into the parenchyma. The main idea of the algorithm is to gradually increase the threshold value of a region-growing until a sudden leakage appears. Afterward, the segmentation that was grown with the last threshold without leakage, is retained.

We have segmented the airway tree from 70 thoracic CT volumes using this method and the proposed one. In volumes acquired at high pressure, the two methods performed similarly, although the proposed method detected slightly longer branches. In images with lower PEEP, the pulmonary parenchyma has higher density and the contrast with the airway lumen may locally increase but leaving still leakages at various sites, therefore methods based on region growing don't perform better. Thanks to the underlying shape model the proposed method was able to better detect small airways, which resulted in more and longer branches compared to the standard method, as illustrated in Fig. 3.

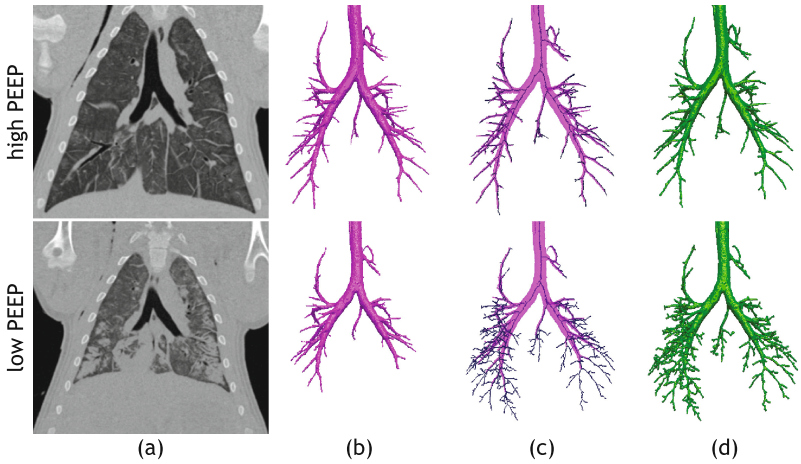

Fig. 3. Qualitative airway segmentation results, (a) Coronal slice of thoracic CT showing the differences in parenchyma intensities between high and low PEEP, (b) result of the reference method, (c) result of the reference method overlayed with a skeleton from the proposed method (d) result of the proposed method.

4.3 Quantitative Evaluation Pipeline

Quantitative evaluation was performed indirectly by comparing two registration-based lung-segmentation methods. The first one used an intensity-driven registration method while the second one used a hybrid registration where intensity information was enriched with airway-tree landmark correspondences. The goal was to test whether the bifurcation and end points obtained from the proposed airway-tree segmentation can improve the lung segmentation in situations where the lung boundary itself does not have sufficient contrast.

To assess registration accuracy, an expert in ARDS was asked to interactively segment the lungs and to mark several anatomical landmarks in the most challenging region of six CT volumes acquired at high, medium and low PEEP. The lung mask segmented by the expert in the image with the best lung boundary contrast (high PEEP), as well as the landmarks in this image, were warped using the transformation field resulting from the registration process between the original image with the highest PEEP and the original image with medium or low PEEP, where the lung is to be automatically segmented.

Registration accuracy was quantitatively evaluated in two ways: (1) the Dice score was calculated between the deformed lung mask of the image with the highest PEEP and the lung mask interactively segmented by the expert in the image with medium or low PEEP, and (2) the residual Euclidean distance was computed, after warping, between corresponding pairs of landmarks.

The landmark correspondences needed to drive the hybrid registration process were obtained from each airway segmentation by first extracting its graph representation [14] where nodes represent bifurcations or end points, and

then by using a matching algorithm proposed in [15]. The latter provides a list of node pairs that match between two airway trees.

4.4 Quantitative Evaluation Results

The accuracy of the registration process is closely related to the number and location of landmark correspondences. Thus, it is important to have accurate airway segmentation with as many branches as possible and without leakages. Therefore, the visual assessment of the segmentation results motivated the use of the proposed method to improve the registration process.

The Dice similarity score for the lung mask segmentation was calculated for the intensity-driven and hybrid registration. For images acquired at high and low PEEP the Dice score was 0.81 for intensity-driven registration and 0.88 for the hybrid registration. Figure 4 visually illustrates these similarities on coronal slices from the posterior region, where the lack of contrast hampered the registration. The main difference is observed in the lowest part of the lung where the hybrid approach reached a better alignment than the intensity-based one. For images acquired at high and medium PEEP, the Dice score was 0.94 for intensity-driven and 0.96 for the hybrid registration.

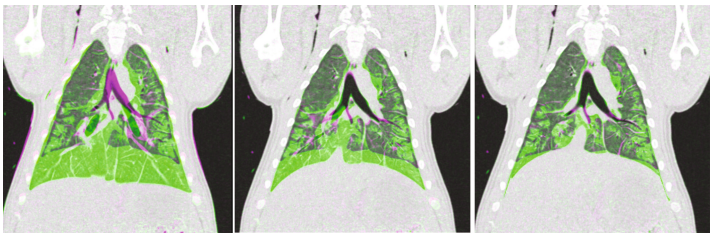

Fig. 4. Coronal slices of moving and fixed images, from the experiment between high PEEP and low PEEP, superposed: before registration (left), after intensity-driven registration (center), and after hybrid registration (right). Color areas correspond to regions where gray levels differ between the images due to lack of alignment and/or to density changes in diseased zones. (Color figure online)

The Euclidean distance between the pairs of manually placed landmarks was calculated between volumes acquired at high and medium PEEP. The average residual distance between the pairs of landmark locations before any transformation was 25.3 mm (range 21.9–29.7 mm). After applying the intensity-based registration and after applying the hybrid registration the average residual distance was 23.5 mm (range 20.4–26.3 mm) and 10.9 mm (range 0.71–29.3 mm), respectively.

Nevertheless, almost the same results (Dice scores and residual distances) were obtained using the reference airway-segmentation method (Mori et al. [1]), within the hybrid registration.

4.5 Computation Time

The proposed algorithm for airway-tree segmentation was implemented in C++. The average running time of a single-threaded implementation was 43 s per thoracic CT volume of mean size $512 \times 512 \times 441$ voxels. The centerline tree extraction took an average time of 41 s, while the onion-kernel region-growing algorithm took an average time of 2 s.

5 Discussion and Conclusions

The method is able to cope with the gray-level diversity in subjects with ARDS that changes with time, mechanical ventilation, and patient position, and it improved lung segmentation by providing landmarks for registration.

Qualitative assessment of the proposed method and the reference method showed that the proposed method detected a larger number of small branches, particularly in poorly-contrasted images acquired at low-pressure conditions. Occasionally, the resulting airway-tree segmentation contained small spurious bulges, caused by a leakage that was stopped by the distance criterion. The distance criterion was set to cover the local neighbourhood that is part of bronchi and at the same time stops the leakage growth already in an early stage. Quantitative evaluation of the proposed method demonstrated that higher number of detected branches yields to automatic extraction of more landmark correspondences between trees from images acquired at different ventilation conditions. This result was used to improve the registration between thoracic CT images from subjects with ARDS, by means of a hybrid approach that uses gray-level correspondences to align well-contrasted structures and landmark correspondences to align regions lacking contrast. The hybrid registration method outperformed gray-level-based registration. Evaluation of the registration serves as an indirect measure of the airway segmentation method because landmark distribution and location strongly depend on the airway-tree segmentation quality.

Although registration results using landmarks from both airways segmentation methods are comparable, this does not devalue the superiority of the proposed method but rather reflects a limitation of the hybrid registration, which would require landmarks in the least contrasted region, where the bronchi are not visible, because they are too thin, and none of the methods can segment them.

In future work, we would like to explore an anatomical evaluation of the approximate centerline tree, based on angles at the bifurcations, to be able to remove the *max_edge_length* criterion. This should allow establishing longer connections between the nodes and, at the same time, the anatomical evaluation will filter out possible spurious branches. The anatomical evaluation will be helpful also for connecting bronchi that are partially filled with mucus and appear disconnected in the CT volumes.

Acknowledgement. The authors thank Dr. Jean-Christophe Richard from team of Réanimation Médicale of the Hôpital de la Croix-Rousse, Lyon, France, for facilitating the images used in this work and helping with the segmentation of the same ones.

K. Lidayová, H. Frimmel, and Ö. Smedby have been supported by the Swedish Research Council (VR), grant no. 621-2014-6153. D. Gómez Betancur has been supported by Colciencias doctoral scholarships program. M. Hernández Hoyos, D. Gómez Betancur, and M. Orkisz were also partly supported by the French-Colombian ECOS Nord grant no. C15M04.

References

1. Mori, K., Hasegawa, J.I., Toriwaki, J.I., Anno, H., Katada, K.: Recognition of bronchus in three-dimensional X-ray CT images with applications to virtualized bronchoscopy system, Proc. 13th Int. Conf. Pattern Recogn. **3**, 528–532 (1996)
2. Wiemker, R., Bülow, T., Lorenz, C.: A simple centricity-based region growing algorithm for the extraction of airways. In: Proceedings of 2nd International Workshop on Pulmonary Image Analysis (MICCAI), pp. 309–314 (2009)
3. van Rikxoort, E.M., van Ginneken, B.: Automated segmentation of pulmonary structures in thoracic computed tomography scans: a review. Phys. Med. Biol. **58**, 187–220 (2013)
4. Pu, J., Gu, S., Liu, S., Zhu, S., Wilson, D., et al.: CT based computerized identification and analysis of human airways: a review. Med. Phys. **39**, 2603–2616 (2012)
5. Aykac, D., Hoffman, E.A., McLennan, G., Reinhardt, J.M.: Segmentation and analysis of the human airway tree from three-dimensional X-ray CT images. IEEE Trans. Med. Imag. **22**(8), 940–950 (2003)
6. Sonka, M., Park, W., Hoffman, E.A.: Rule-based detection of intrathoracic airway trees. IEEE Trans. Med. Imaging **15**(3), 314–326 (1996)
7. Bartz, D., Mayer, D., Fischer, J., Ley, S., del Rio, A., Thust, S., Straßr, W.: Hybrid segmentation and exploration of the human lungs. In: Visualization, pp. 177–184. IEEE (2003)
8. Lo, P., Sporring, J., Ashraf, H., Pedersen, J.J., de Bruijne, M.: Vessel-guided airway tree segmentation: a voxel classification approach. Med. Image Anal. **14**(4), 527–538 (2010)
9. Li, Q., Sone, S., Doi, K.: Selective enhancement filters for nodules, vessels, and airway walls in two-and three-dimensional CT scans. Med. Phys. **30**(8), 2040–2051 (2003)
10. Lo, P., van Ginneken, B., Reinhardt, J.M., Tarunashree, Y., et al.: Extraction of airways from CT (EXACT'09). IEEE Trans. Med. Imaging. **31**, 2093–2107 (2012)
11. Lidayová, K., Frimmel, H., Wang, C., Bengtsson, E., Smedby, Ö.: Fast vascular skeleton extraction algorithm. Pattern Recogn. Letters **76**, 67–75 (2016)
12. Gattinoni, L., Caironi, P., Pelosi, P., Goodman, L.R.: What has computed tomography taught us about the acute respiratory distress syndrome? Am. J. Respir. Crit. Care Med. **164**(9), 1701–1711 (2001)
13. Frimmel, H., Näppi, J., Yoshida, H.: Centerline-based colon segmentation for CT colonography. Med. Phys. **32**(8), 2665–2672 (2005)
14. Flórez-Valencia, L., Morales Pinzón, A., et al.: Simultaneous skeletonization and graph description of airway trees in 3D CT images. In: Proceedings of 25th GRETSI (2015)
15. Morales Pinzón, A., Hernández Hoyos, M., Richard, J.C., Flórez-Valencia, L., Orkisz, M.: A tree-matching algorithm: application to airways in CT images of subjects with the acute respiratory distress syndrome. Med. Image Anal. **35**, 101–115 (2017)